

MotionAgent: Fine-grained Controllable Video Generation via Motion Field Agent

Xinyao Liao^{1,2} Xianfang Zeng^{2*} Liao Wang³ Gang Yu^{2†} Guosheng Lin^{1†} Chi Zhang⁴
¹Nanyang Technological University ²StepFun ³ShanghaiTech University ⁴Westlake University

Abstract

We propose *MotionAgent*, enabling fine-grained motion control for text-guided image-to-video generation. The key technique is the motion field agent that converts motion information in text prompts into explicit motion fields, providing flexible and precise motion guidance. Specifically, the agent extracts the object movement and camera motion described in the text and converts them into object trajectories and camera extrinsics, respectively. An analytical optical flow composition module integrates these motion representations in 3D space and projects them into a unified optical flow. An optical flow adapter takes the flow to control the base image-to-video diffusion model for generating fine-grained controlled videos. The significant improvement in the Video-Text Camera Motion metrics on VBench indicates that our method achieves precise control over camera motion. We construct a subset of VBench to evaluate the alignment of motion information in the text and the generated video, outperforming other advanced models on motion generation accuracy.

1. Introduction

Recently, image-to-video (I2V) generation models [4, 6, 9, 12, 21, 29, 30, 37, 54, 60, 66, 68] develop rapidly. These models bring images to life, making the visual content more dynamic and vivid. Compared to text-to-video (T2V) generation models [2, 5, 11, 13, 15–17, 31, 40], I2V models use an image as the reference, which further constrains the content and reduces the uncertainty of the generated video. Most existing I2V generation models already achieve high-quality video generation, allowing them to preserve the visual details of the input image while generating stable results. However, precise control over the video using only text input remains a field worth exploring.

Some I2V generation models [4, 12] randomly make the input image dynamic, resulting in an uncontrollable gener-

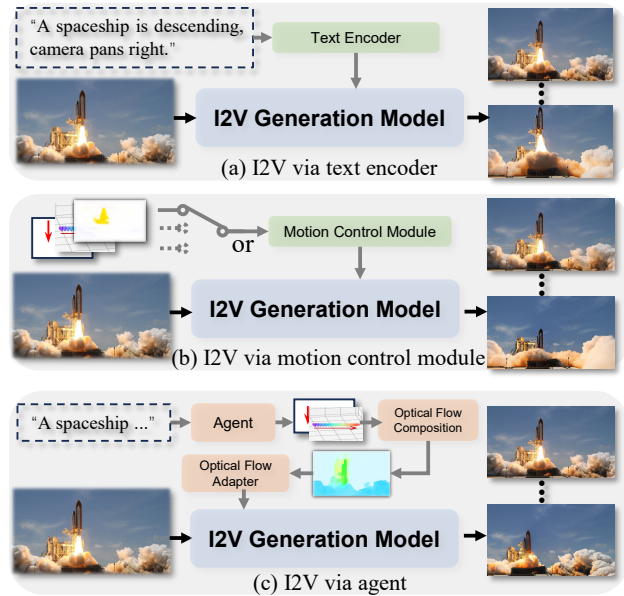


Figure 1. Different frameworks of I2V generation models. (a) Controllable I2V generation via text encoder. (b) Controllable I2V generation via special control module. (c) Our method, controllable I2V generation via motion field agent.

ated result. Other I2V models [9, 29, 30, 37, 54, 66, 68] support simple control through text input. As shown in Figure 1(a), they adopt a text encoder to inject control information into visual features. They can perform overall control, but it is difficult to achieve fine-grained control over each element of the video. Additionally, training an I2V generation model with high alignment between motion information in the text and the video relies heavily on the quality of training data [3, 7, 42, 49, 58], and obtaining high-quality training data is also labor-intensive.

As illustrated in Figure 1(b), some controllable I2V generation models adopt specially designed modules for controlling different motion types, such as object movement [32, 50–52, 61, 69, 71] or camera motion [14, 55, 56]. These modules are proposed for individual control conditions, making it difficult to control multiple motion types

*Xianfang Zeng is the project leader.

†Corresponding authors: skicy@outlook.com, gslin@ntu.edu.sg

simultaneously. Additionally, inputting these control conditions may require expert knowledge, which creates a barrier for non-professional users. These methods are less flexible than those that directly control video motion through text input.

To this end, we propose MotionAgent, which enables fine-grained control for text-guided I2V generation. The key design is the motion field agent that converts the motion information in the text prompts into explicit motion representations, providing precise motion guidance. As shown in Figure 1(c), our framework directly takes the text as input. First, the agent parses and converts the motion information in the text into object trajectories and camera extrinsics, which explicitly represent object movement and camera motion, respectively. Then, these two intermediate representations are integrated in the 3D space and projected into unified optical flow maps through the proposed analytical optical flow composition module. Finally, we tune an optical flow adapter, using the unified flow as conditions, to control a base I2V diffusion model for video generation.

In the experiments, we first evaluate our method on a public I2V generation benchmark [20]. Evaluation results demonstrate that our approach significantly improves the control accuracy of camera motion and achieves comparable video quality with other advanced models. Furthermore, we construct a subset of VBench for assessing the alignment of motion information in the text and the generated video. The results illustrate that our method achieves the best motion accuracy. We also conduct a user study, which shows that our generated videos align better with the motion information in the text and maintain high quality. Finally, we conduct ablation studies to verify the effectiveness of the proposed components. Our contributions can be summarized as follows:

- We propose a novel I2V generation pipeline via a motion field agent, which enables fine-grained motion control for text-guided image-to-video generation.
- We construct a new video motion benchmark, a subset of VBench, to assess the alignment of fine-grained motion information in the text and the generated video.
- Extensive experiments demonstrate the effectiveness of our proposed method which achieves the most accurate motion control in I2V generation with only text input.

2. Related Work

2.1. Video Generation via Agent

The development of ChatGPT [34] and GPT-4 [1] represents a crucial advancement in natural language processing. These large language models (LLMs) [26, 43, 48, 63, 67] enable multi-round conversations and have the impressive ability to follow complex instructions. Furthermore, the integration of vision capabilities in GPT-4V [59] is a mile-

stone, enabling LLMs to process and interpret multimodal data. The vision capabilities in LLMs pave the way for the development of multimodal LLM-powered agents. These agents increasingly gain attention for their ability to effectively handle multimodal inputs and achieve complex tasks.

A series of studies propose to exploit the knowledge of agents for achieving controllable generation [10, 24, 25], zero-shot generation [18, 19, 28, 33], or long video generation [47, 72]. Anim-Director [22] builds an autonomous animation-making agent for generating contextually coherent animation videos. DreamFactory [53] leverages multi-agent collaboration principles and a keyframe iteration method to ensure consistency and style across long videos. VIDEOAGENT [41] aims to improve video plan generation based on a feedback pipeline. ChatCam [27] introduces a system that navigates camera motion through conversations with users and mimics a professional cinematographer’s workflow.

Our research contributes to this area by proposing a motion field agent to decompose and convert the motion information in the text into explicit intermediate representations of object movement and camera motion to guide precise control over video generation.

2.2. Text-guided I2V Generation

Generally, most I2V generation models [9, 21, 29, 66] support text and image input simultaneously. The input image guides the visual content of the video, while the text indicates the potential motion. VideoCrafter [6], Dynamicrafter [54], ConsistI2V [37], and I2VGen-XL [68] are all based on the U-Net [38] backbone and use a text encoder to inject text embeddings into visual features, enabling text control over video content. CogVideoX [60] and OpenSora [45], based on the DIT [35] architecture, gain control capability by jointly learning text tokens and visual tokens. These methods, which directly learn the similarity between text embeddings and visual features, often highly depend on the quality of training data. However, there is a lack of large high-quality datasets with text labels that describe video motion. The text labels in most video datasets [3, 7, 42, 49, 58] describe the content of a frame without much motion information and are not suitable for training I2V generation models with strong motion control capability, which leads to poor performance of these methods in achieving precise motion control through direct text input.

2.3. I2V Generation via Motion Control Module

With the development of video generation models, controllable video generation gradually attracts more attention. Existing methods [55, 56, 69] propose designing specialized modules for certain motion types, such as object movement or camera motion. DragNUWA [61] encodes sparse point trajectories into dense features as guidance informa-

tion, which is then injected into the diffusion model to control object motion. DragAnything [52] uses masks to identify a central point and subsequently generates a Gaussian map to track this center, providing a guiding trajectory for object-controllable I2V generation. TrackGo [71] introduces a TrackAdapter, which encodes object trajectories into the network through a dual attention mechanism to control object movement in the generated videos. Other video generation methods achieve control of camera motion. MotionCtrl [50] directly encodes camera extrinsics as features and inputs them to the model. IMAGE CONDUCTOR [23] and CameraCtrl [14] both convert sparse camera extrinsics into dense feature maps using Plücker embeddings and employ these dense embeddings to control camera motion.

In addition to encoding control conditions into deep features, some methods generate explicit intermediate representations, such as optical flow, to control the generated video. Motion-I2V [39] factorizes I2V generation into two stages: It first generates optical flow maps using a flow diffusion model and then uses the optical flow maps as explicit motion guidance for video generation. MOFA-Video [32] proposes a generative motion field adapter. They first convert sparse point trajectories into dense optical flow through a sparse-to-dense network and then use an optical flow adapter to control video generation. Although these models achieve control over the videos via a motion control module, and their control capabilities are stronger than those of text-based models, they often require specific knowledge, such as providing object trajectories or camera extrinsics, which creates a barrier for users. Moreover, most controllable I2V generation methods can only control a single motion type at a time and struggle to achieve simultaneous control of all types.

Our method leverages the optical flow adapter proposed by MOFA-Video [32] to control the base I2V diffusion model. Unlike MOFA-Video, our approach has two differences: 1) We propose a motion field agent that allows direct control of the generated video through text input rather than manual trajectory plotting. 2) We introduce an analytical optical flow composition module, which enables our method to simultaneously control both object movement and camera motion.

3. Method

Our method aims to achieve fine-grained controllable I2V generation through text input, allowing precise control of both object movement and camera motion. Specifically, a motion field agent first converts the motion information in the text into object trajectories and camera extrinsics. These two explicit intermediate representations are then fed into an improved controllable I2V generation model to guide the video generation. Within the controllable I2V generation model, the object trajectories and camera extrinsics are

integrated by an analytical optical flow composition module to compute unified optical flow maps. Subsequently, we employ Stable Video Diffusion (SVD) [4] as the base I2V diffusion model and utilize an optical flow adapter [32] as the motion control module to generate the final video.

3.1. Motion Field Agent

As for the motion field of a video, we generally decompose it into object movement within the frame and overall camera motion. Based on the above decomposition, our agent performs two key tasks: object trajectory plotting and camera extrinsics generation. The details of the designed agent can be found in Figure 2.

3.1.1. Video Motion Decomposition

The agent analyzes motion information in the text and splits it into parts that respectively describe object movement and camera motion. This step decouples the complex motion information, allowing for precise and independent control of each motion type.

3.1.2. Object Trajectory Plotting

The object trajectory plotting step can be divided into two sub-tasks: object identification and trajectory plotting.

Object Identification: (1) The agent first splits the text of object movement into independent descriptions of each object shown in the given image. (2) Then, the agent further finds the dynamic object described in the text and feeds it into an open-world object detection algorithm. (3) The Grounded-SAM [36] model is called for auxiliary detection and segmentation, facilitating the agent in identifying the corresponding object in the input images. All detection and segmentation results are plotted on the image as semi-transparent masks, which are fed back into the agent for identifying the object.

Trajectory Plotting: (4) The agent locates the object in the image based on the detection and segmentation results, thereby determining the starting point of the trajectory. (5) The agent plots the trajectory with varying lengths and curvature according to the complexity of the text description.

To enhance the capabilities of trajectory plotting, we replace direct trajectory generation with a grid selection approach [65]. An image is divided into $N \times M$ grids, with each grid labeled by an integer. The agent determines each point of the trajectory by selecting grid numbers, and the trajectory is formed by sequentially connecting all the points. More details of trajectory plotting can be found in the supplementary material.

3.1.3. Camera Extrinsics Generation

Agent directly generates camera extrinsics E based on the text of camera motion and the input image. The text description specifies the motion type, such as zoom in/out, pan

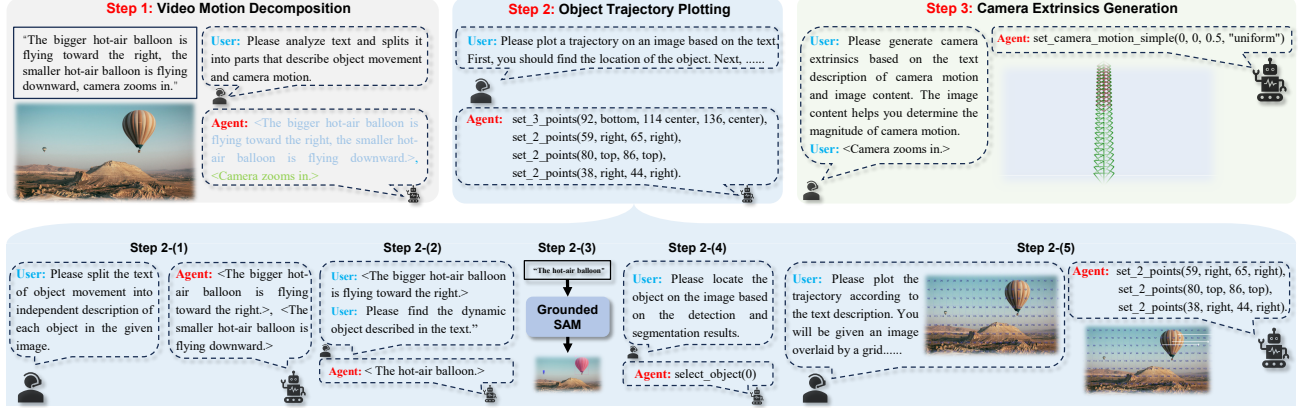


Figure 2. Pipeline of Motion Field Agent. **Step 1:** The agent first parses the input text, dividing the motion information into two parts that respectively describe object movement and camera motion. **Step 2:** The agent draws the object trajectories according to the text of object movement. **Step 3:** The agent directly generates the camera extrinsics based on the text of camera motion.

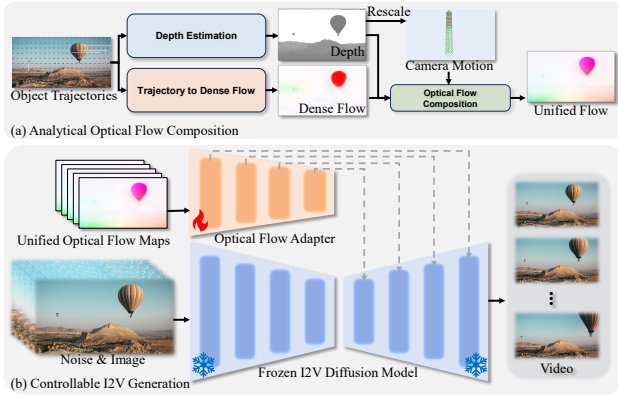


Figure 3. Controllable I2V Generation Model. (a) The analytical optical flow composition module calculates unified optical flow maps based on the object trajectories and camera extrinsics. (b) The unified flow maps are fed into a fine-tuned optical flow adapter as the control condition. Then, we generate precisely controlled video results based on a base I2V diffusion model.

left/right, and tilt up/down. The image helps the agent determine the magnitude of the camera motion. For instance, a wide landscape scene may require intensive camera motion, while a narrow close-up shot may only need slight adjustments of camera location. It is worth noting that we constrain the translation T of the camera extrinsics to $(-1, 1)$. In the next analytical optical flow composition module, we rescale the translation T back to a reasonable range based on the estimated depth map.

3.2. Controllable I2V Generation

After the agent converts the motion information in the text into object trajectories and camera extrinsics, our improved controllable I2V generation model uses these two intermediate representations as inputs, enabling fine-grained con-

trol of object movement and camera motion in the video.

3.2.1. Analytical Optical Flow Composition

As shown in Figure 3(a), this module employs optical flow as a proxy to geometrically compose object movement and camera motion, enabling our I2V generation model to accurately control each motion type in a unified manner.

We first use Metric3D [62] to estimate the depth map D of the input image and unproject each pixel I^0 in the image to obtain the 3D location P .

CMP [64] is utilized to estimate the dense optical flow of object movement F_{obj} according to the sparse object trajectories. Based on the estimated optical flow F_{obj} and the depth map D , we calculate the 3D location offset O caused by object movement. Note that we assume a large focal length for all images, thereby neglecting the offset on the z -axis, where $o_z = 0$. We simply assume that the 3D location offset of the i -th pixel on the x/y -axis o_{xy}^i is proportional to its depth d^i , with the same direction as the corresponding optical flow f_{obj}^i . It can be formulated as,

$$o_{xy}^i = K^{-1} \cdot f_{obj}^i \cdot d^i, \quad (1)$$

where K is the camera intrinsics.

Then, we apply the offset on the x/y -axis o_{xy}^i to the 3D location of i -th pixel p_{xy}^I , which can be computed as,

$$\hat{p}_{xy}^i = p_{xy}^I + o_{xy}^i, \quad (2)$$

where \hat{p}_{xy}^i is the new 3D location of i -th pixel on the x/y -axis, and $\hat{p}_z^i = p_z^i$.

We rescale the translation T of the camera extrinsics E according to the maximum depth range. Subsequently, we reproject these moved points \hat{P} into the corresponding image coordinate systems based on the camera extrinsics E^t

to calculate the new pixel position I^t in the t -th frame. It can be calculated as,

$$I^t = \Pi(E^t \hat{P}), \quad (3)$$

where, E^t is the camera extrinsics of the t -th frame, and Π is the projection operation. We assume that the camera coordinate of the first frame serves as the world coordinate.

Finally, we calculate the pixel offsets of the corresponding pixel points, which can be noted as,

$$\bar{F}^t = I^t - I^0, \quad (4)$$

where \bar{F} are named unified optical flow maps. These flow maps contain motion information of both object movement and camera motion.

Figure 3(b) illustrates the process of controllable I2V generation according to the unified optical flow maps. By adopting the unified optical flow maps as the control conditions, we leverage the optical flow adapter proposed by MOFA-Video [32] and the frozen I2V diffusion model SVD [4] to achieve controllable I2V generation.

3.2.2. Optical Flow Adapter Tuning

Since the unified optical flow maps involve many simplifications and approximations, they contain geometrically unrealistic regions compared to the true optical flow maps. Directly using these flow maps as input for the optical flow adapter, which is trained on real optical flow maps, may lead to degraded results in the generated videos. We propose fine-tuning the optical flow adapter on the unified optical flow maps.

For each training video, we first use an optical flow model, Unimatch [57], to estimate the real optical flow. Then we employ a SLAM method, DROID-SLAM [46], to compute the camera extrinsics for each frame. Next, we eliminate the optical flow caused by camera motion based on the estimated camera extrinsics, and approximately obtain the optical flow caused by object movement. We perform sparse sampling [64] on these optical flow maps to obtain sparse object trajectories. More details of data preparation can be found in the supplementary material. Subsequently, we reuse the proposed analytical composition method to calculate the unified optical flow maps, which are utilized as input to fine-tune the optical flow adapter. This step eliminates the domain gap between real and unified flow fields and facilitates high-quality video results.

4. Experiments

We provide extensive comparisons to evaluate our models on controllable I2V generation tasks. First, we introduce the implementation details and evaluation metrics (Sec. 4.1). Importantly, we show the results on the general I2V generation benchmark (Sec. 4.2.1), controllable I2V generation

benchmark (Sec. 4.2.2), and user study (Sec. 4.2.3). Lastly, we conduct ablation studies to demonstrate the effectiveness of each module in our MotionAgent (Sec. 6.1).

4.1. Implementation Details

For the motion field agent, we adopt GPT-4o [1] as the LLM. We input the image with a resolution of 2560×1600 to the agent. In the trajectory plotting module, we divide the image into 20×10 grids. For controllable I2V generation, we tune the optical flow adapter module on 32 NVIDIA A800 GPUs. The frozen base I2V generation model is SVD [4]. We use AdamW as an optimizer. During training, we randomly sample 24 video frames with a stride of 4. The learning rate is set to 2×10^{-5} with a resolution of 512×512 .

Metrics. In the comparison experiments of the general I2V generation task, we adopt the same evaluation metrics introduced by VBench [20]. In the comparison of controllable I2V generation, we report Object Movement Q&A, Complex Camera Motion, and Overall Score.

I2V Score reports the overall score of I2V generation metrics. Video-Text Camera Motion assesses the consistency between camera motion and the input text, such as zoom in/out. Video-Image Subject Consistency assesses whether the appearance of the subject remains consistent throughout the entire video compared to the input image. Video-Image Background Consistency evaluates the temporal consistency of background scenes with the input image. Subject Consistency assesses whether the subject’s appearance remains consistent throughout the entire video. Background Consistency evaluates the temporal consistency of the background scenes across frames. Motion Smoothness evaluates whether the motion in the generated video is smooth and follows the physical laws of the real world. Aesthetic Quality evaluates the artistic and aesthetic value perceived by humans towards each video frame. Dynamic Degree evaluates the level of dynamics generated by each model. Object Movement Q&A assesses the consistency between the text description and object movement in the video. Complex Camera Motion evaluates the consistency between complex camera movements in the generated video and the input text description. Total Score is the overall metric of controllable I2V generation. All evaluation metrics are higher-the-better.

4.2. Comparison with other SOTA Methods

4.2.1. General I2V Generation

We evaluate the general I2V generation capabilities on a public video generation benchmark, VBench [20]. We compare our model with existing I2V generation models, including VideoCrafter [6], ConsistI2V [37], SEINE [8], I2VGen-XL [68], Animate-Anything [9], DynamiCrafter [54], and our base I2V diffusion model SVD [4]. To ensure a fair comparison of general I2V generation, we di-

Method	I2V Score	Video-Text Camera Motion	Video-Image Subject Consistency	Video-Image Background Consistency	Subject Consistency	Background Consistency	Motion Smoothness	Aesthetic Quality	Dynamic Degree
VideoCrafter [6]	88.95	33.60	91.17	91.31	<u>97.86</u>	98.79	98.00	60.78	22.60
ConsistI2V [37]	94.81	<u>33.92</u>	95.82	95.95	95.27	<u>98.28</u>	97.38	59.00	18.62
SEINE [8]	96.26	20.97	97.15	96.94	95.28	97.12	97.12	64.55	<u>27.07</u>
I2VGen-XL [68]	96.98	13.00	97.52	97.68	<u>96.36</u>	97.93	<u>98.31</u>	<u>65.33</u>	24.96
Animate-Anything [9]	98.31	13.08	98.76	<u>98.58</u>	98.90	<u>98.19</u>	<u>98.61</u>	67.12	2.68
DynamiCrafter [54]	<u>97.98</u>	<u>35.81</u>	<u>98.17</u>	98.60	95.69	<u>97.38</u>	97.38	<u>66.46</u>	47.40
SVD [4]	96.93	-	97.51	97.62	95.42	96.77	98.12	60.23	<u>43.17</u>
MotionAgent (Ours)	<u>97.51</u>	81.91	<u>98.06</u>	<u>98.00</u>	96.10	96.76	98.93	64.48	16.67

Table 1. Evaluation results of general I2V generation on VBench [20] (all values are in percentage). The best result is indicated in **bold**, the second-best result is indicated with underlines, and the third-best result is indicated with double underlines.

rectly use the images and original text prompts provided by VBench as inputs for our model. The evaluation results of other methods are taken directly from the leaderboard on the official website [44].

As shown in Table 1, our method maintains high-quality I2V generation capabilities. Our pipeline ranks among the top for most metrics and even achieves the best results for some. These results demonstrate that our model can be compatible with general text prompts that may do not include motion information.

Compared with the base model SVD [4], our method shows better results in consistency, smoothness, and aesthetic quality metrics. These improvements are attributed to the motion field agent, which can reason and generate suitable object trajectories and camera motion even when there is no motion information included in the text prompts. Additionally, the tuning of the optical flow adapter also improves video quality by constraining the generated video with optical flow and eliminating unreasonable motion. The dynamic degree metric of our method decreases due to the precise control we implement over the generated video. The objects mentioned in the text move accurately, while those not mentioned remain as static as possible, which leads to a lower dynamic degree score. When our model is given a detailed text description with more motion information, it can generate videos with a higher dynamic degree.

Notably, our method achieves 81.91% for the Video-Text Camera Motion metric, which is significantly higher than other methods. This result demonstrates that our method achieves precise control over camera motion according to the text input. The base model SVD does not support text input, while our approach enables SVD to control generated video through text input.

4.2.2. Controllable I2V Generation

To further evaluate the control capabilities of I2V generation models through direct text input, we conduct additional assessments. Currently, existing video generation benchmarks do not specifically evaluate the alignment of motion information in the text prompts and the video, so we introduce a new benchmark to evaluate the semantic alignment

Method	Object Movement Q&A	Complex Camera Motion	Total Scores
VideoCrafter [6]	13.67	6.64	9.42
ConsistI2V [37]	24.57	6.03	13.35
SEINE [8]	21.99	1.66	9.69
Motion-I2V [39]	28.76	7.09	15.65
DynamiCrafter [54]	<u>29.38</u>	<u>8.22</u>	<u>16.58</u>
CogVideoX [60]	26.47	<u>20.62</u>	<u>22.93</u>
Pyramid Flow [21]	<u>30.96</u>	6.18	15.97
MotionAgent (Ours)	45.69	77.76	65.10

Table 2. Evaluation results of controllable I2V generation on our benchmark (all values are in percentage). The best result is indicated in **bold**, the second-best result is indicated with underlines, and the third-best result is indicated with double underlines.

between videos and input text.

We reuse images from VBench [20] and add more motion information to the original text prompts. To evaluate the control capabilities of object movement, we design new text prompts for 83 images from VBench, providing detailed object movement descriptions. For camera motion, we modify the simple camera motion prompts of 109 images to more complex ones, such as changing “zoom in” to “first zoom in then zoom out” or “zoom in incrementally.”

For each text prompt describing object movement, we design corresponding questions. We utilize a multimodal LLM model, GPT-4o [34], to score the semantic alignment between the object movement in the videos and the input text through a question-and-answer (Q&A) approach. To evaluate complex camera motions, we adopt the evaluation method introduced by VBench. The compared methods include five UNet-based models: VideoCrafter [6], ConsistI2V [37], SEINE [8], Motion-I2V [39], and DynamiCrafter [54]; and two DIT-based models: CogVideoX [60] and Pyramid Flow [21].

As shown in Table 2, our method achieves the best results compared to other methods in controllable video generation tasks. For the Object Movement Q&A metric, our method demonstrates stronger control over object movement, with higher accuracy scored by GPT-4o [34]. It is worth noting that current multimodal LLMs have limited

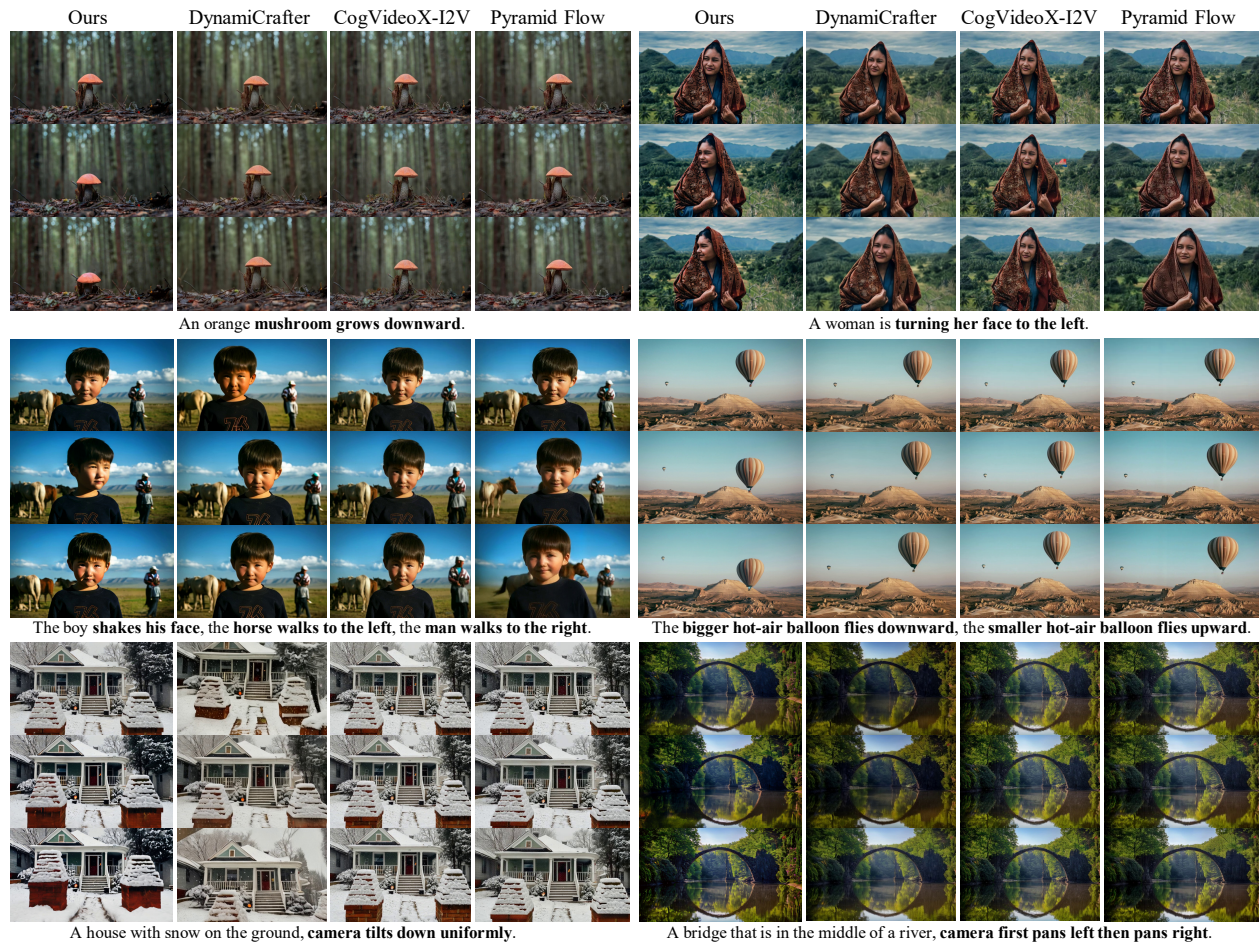


Figure 4. Comparison results of controllable I2V generation on our benchmark. The motion described in the text is in **bold**.

reasoning capabilities, which may lead to some inaccurate judgments and responses. However, the numerical results still indicate that our method achieves the most accurate control over object movement. For the Complex Camera Motion metric, our method significantly outperforms the other methods. Compared to Motion-I2V [39], the optical flow generated by the motion field agent represents the motion information more precisely and results in a higher total score. Moreover, our method maintains consistent performance regardless of whether the camera motion is simple or complex, as illustrated by the camera motion metrics in Tables 1 and 2. Some qualitative comparison results are shown in Figure 4, where our method showcases more precise control over generated videos.

Our method directly converts motion information in the text prompts into the intermediate motion representations through the motion field agent, and then uses optical flow to achieve controllable video generation. Without needing high-quality video-image-text pair training data, our approach achieves fine-grained controllable I2V generation.

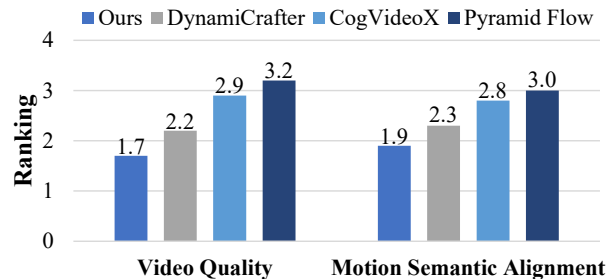


Figure 5. User study results of controllable I2V generation on video quality and semantic alignment of the motion information in text prompt and video.

4.2.3. User Study

We collect 30 images from VBench [20] and expand the prompts by adding detailed descriptions of object movement and camera motion. We then generate videos using the official codes of DynamiCrafter [54], CogVideoX [60], and Pyramid Flow [21]. The user study is expected to be

Detection Tool	Object Movement	Camera Motion	Flow Composition	Object Movement Q&A	Complex Camera Motion	Dynamic Degree
	✓	✓	✓	34.33	75.11	20.53
✓	✓		✓	38.20	0.30	29.95
✓		✓	✓	10.51	75.95	8.42
✓	✓	✓		30.07	64.92	27.89
✓	✓	✓	✓	45.69	77.76	32.11

Table 3. Ablation study of object identification module and optical flow composition module on our benchmark (all values are in percentage).

completed in 10-20 minutes. For each case, the user study interface shows the videos generated by four methods, and participants are instructed to evaluate the videos from two dimensions: (i) “Please sort the videos by visual quality from best to worst.”; (ii) “Please sort the videos from high to low based on the semantic alignment of the motion information in the text prompt and the video.”. Finally, we receive 50 valid responses from the participants.

As illustrated in Figure 5, our method achieves the top rank in both dimensions. These results demonstrate that our method generates high-quality videos with the best alignment of motion information in the text.

4.3. Ablation Study

4.3.1. Object Identification

We conduct an ablation study on the approach to identify the objects described in the text. In our method, we use Grounded-SAM [36] as an auxiliary detection algorithm to help the agent locate the corresponding objects. Here, we also propose a detection-free approach to achieve object identification through multiple rounds of dialogue.

Specifically, we first ask the agent to determine an initial position, which represents the object described in the text. Then, we plot this initial position directly on the image and input it again along with the text description to the agent. If the agent considers the current initial position correct, it returns the current position directly. If the agent considers the current position incorrect, it returns a new position. The dialogue loop continues until the agent confirms the correctness of the last selected position.

We compare the two approaches for identifying the objects described in the text. As shown in Table 3, the results using Grounded-SAM (full model) are significantly better than those using the multi-round dialogue (without a detection tool). The multi-round dialogue leads to some incorrect judgments, resulting in a lower score on the Object Movement Q&A metric. Additionally, our method decomposes object movement and camera motion, so the degradation caused by incorrect object identification does not significantly affect the camera motion in the generated video. Moreover, the misjudgments in object identification lead to the degradation of the dynamic degree metric.

4.3.2. Optical Composition

Then, we conduct an ablation study on the analytical optical flow composition module and use the original generative motion field adapter proposed by MOFA-Video [32] as a baseline. The baseline can only control object movement or camera motion independently, so we define two models: “without camera motion” and “without object movement,” which represent models that can only control either object movement or camera motion independently.

In our proposed module, we design an approach to compose optical flow using an analytical method. To verify the effectiveness of this approach, we design a mechanism that directly adds the optical flow of object movement and the optical flow caused by camera motion, which we call “without flow composition.”

As shown in Table 3, the baseline models can only control object movement or camera motion independently. Compared to “without flow composition,” our proposed analytical optical flow composition module achieves higher scores on both the Object Movement Q&A and Complex Camera Motion metrics. Directly adding optical flows results in many unreasonable areas in the added flow maps, and the object optical flow may be overshadowed by the camera optical flow. For the dynamic degree metric, our full module also achieves the highest scores. Moreover, the dynamic degree results are higher than those acquired from the original prompts in VBench [20]. This showcases that our method generates videos with a higher dynamic degree when there is more detailed motion information in the given text, and follows the text instructions accurately.

5. Conclusion

This work aims to address the challenge of precisely controlling I2V generation using only text input. We first propose a motion field agent that converts the motion information in the text into object trajectories and camera extrinsics. Then, we design an analytical optical flow composition module to integrate the explicit motion representations into unified optical flow maps. Next, we fine-tune an optical flow adapter to achieve controllable I2V generation. In the experiments, we construct a new video motion benchmark, and the evaluation results demonstrate that our method significantly outperforms other text-guided I2V generation models.

Limitation. Due to the limited reasoning capabilities of LLMs, our method may fail to understand particularly complex motions. In these cases, the object trajectories and camera extrinsics generated by the motion field agent may be unreasonable. In future work, we can address these problems by constructing text-motion pairs and fine-tuning the LLMs to enhance their ability to understand particularly complex motions.

References

- [1] Josh Achiam, Steven Adler, Sandhini Agarwal, Lama Ahmad, Ilge Akkaya, Florencia Leoni Aleman, Diogo Almeida, Janko Altenschmidt, Sam Altman, Shyamal Anadkat, et al. Gpt-4 technical report. *arXiv preprint arXiv:2303.08774*, 2023. 2, 5
- [2] Jie An, Songyang Zhang, Harry Yang, Sonal Gupta, Jia-Bin Huang, Jiebo Luo, and Xi Yin. Latent-shift: Latent diffusion with temporal shift for efficient text-to-video generation. *arXiv preprint arXiv:2304.08477*, 2023. 1
- [3] Max Bain, Arsha Nagrani, Gül Varol, and Andrew Zisserman. Frozen in time: A joint video and image encoder for end-to-end retrieval. In *Proceedings of the IEEE/CVF international conference on computer vision*, pages 1728–1738, 2021. 1, 2
- [4] Andreas Blattmann, Tim Dockhorn, Sumith Kulal, Daniel Mendelevitch, Maciej Kilian, Dominik Lorenz, Yam Levi, Zion English, Vikram Voleti, Adam Letts, et al. Stable video diffusion: Scaling latent video diffusion models to large datasets. *arXiv preprint arXiv:2311.15127*, 2023. 1, 3, 5, 6
- [5] Andreas Blattmann, Robin Rombach, Huan Ling, Tim Dockhorn, Seung Wook Kim, Sanja Fidler, and Karsten Kreis. Align your latents: High-resolution video synthesis with latent diffusion models. In *Proceedings of the IEEE/CVF Conference on Computer Vision and Pattern Recognition*, pages 22563–22575, 2023. 1
- [6] Haoxin Chen, Menghan Xia, Yingqing He, Yong Zhang, Xiaodong Cun, Shaoshu Yang, Jinbo Xing, Yaofang Liu, Qifeng Chen, Xintao Wang, et al. Videocrafter1: Open diffusion models for high-quality video generation. *arXiv preprint arXiv:2310.19512*, 2023. 1, 2, 5, 6
- [7] Tsai-Shien Chen, Aliaksandr Siarohin, Willi Menapace, Ekaterina Deyneka, Hsiang-wei Chao, Byung Eun Jeon, Yuwei Fang, Hsin-Ying Lee, Jian Ren, Ming-Hsuan Yang, et al. Panda-70m: Captioning 70m videos with multiple cross-modality teachers. In *Proceedings of the IEEE/CVF Conference on Computer Vision and Pattern Recognition*, pages 13320–13331, 2024. 1, 2
- [8] Xinyuan Chen, Yaohui Wang, Lingjun Zhang, Shaobin Zhuang, Xin Ma, Jiashuo Yu, Yali Wang, Dahua Lin, Yu Qiao, and Ziwei Liu. Seine: Short-to-long video diffusion model for generative transition and prediction. In *The Twelfth International Conference on Learning Representations*, 2023. 5, 6
- [9] Zuozhuo Dai, Zhenghao Zhang, Yao Yao, Bingxue Qiu, Siyu Zhu, Long Qin, and Weizhi Wang. Animateanything: Fine-grained open domain image animation with motion guidance. *arXiv e-prints*, pages arXiv–2311, 2023. 1, 2, 5, 6
- [10] Weixi Feng, Wanrong Zhu, Tsu-jui Fu, Varun Jampani, Arjun Akula, Xuehai He, Sugato Basu, Xin Eric Wang, and William Yang Wang. Layoutgpt: Compositional visual planning and generation with large language models. *Advances in Neural Information Processing Systems*, 36, 2024. 2
- [11] Songwei Ge, Seungjun Nah, Guilin Liu, Tyler Poon, Andrew Tao, Bryan Catanzaro, David Jacobs, Jia-Bin Huang, Ming-Yu Liu, and Yogesh Balaji. Preserve your own correlation: A noise prior for video diffusion models. In *Proceedings of the IEEE/CVF International Conference on Computer Vision*, pages 22930–22941, 2023. 1
- [12] Xun Guo, Mingwu Zheng, Liang Hou, Yuan Gao, Yufan Deng, Pengfei Wan, Di Zhang, Yufan Liu, Weiming Hu, Zhengjun Zha, et al. I2v-adapter: A general image-to-video adapter for diffusion models. In *ACM SIGGRAPH 2024 Conference Papers*, pages 1–12, 2024. 1
- [13] Yuwei Guo, Ceyuan Yang, Anyi Rao, Zhengyang Liang, Yaohui Wang, Yu Qiao, Maneesh Agrawala, Dahua Lin, and Bo Dai. Animatediff: Animate your personalized text-to-image diffusion models without specific tuning. *arXiv preprint arXiv:2307.04725*, 2023. 1
- [14] Hao He, Yinghao Xu, Yuwei Guo, Gordon Wetzstein, Bo Dai, Hongsheng Li, and Ceyuan Yang. Cameractrl: Enabling camera control for text-to-video generation. *arXiv preprint arXiv:2404.02101*, 2024. 1, 3
- [15] Yingqing He, Tianyu Yang, Yong Zhang, Ying Shan, and Qifeng Chen. Latent video diffusion models for high-fidelity long video generation. *arXiv preprint arXiv:2211.13221*, 2022. 1
- [16] Jonathan Ho, William Chan, Chitwan Saharia, Jay Whang, Ruiqi Gao, Alexey Gritsenko, Diederik P Kingma, Ben Poole, Mohammad Norouzi, David J Fleet, et al. Imagen video: High definition video generation with diffusion models. *arXiv preprint arXiv:2210.02303*, 2022.
- [17] Jonathan Ho, Tim Salimans, Alexey Gritsenko, William Chan, Mohammad Norouzi, and David J Fleet. Video diffusion models. *Advances in Neural Information Processing Systems*, 35:8633–8646, 2022. 1
- [18] Susung Hong, Junyoung Seo, Heeseong Shin, Sunghwan Hong, and Seungryong Kim. Direct2v: Large language models are frame-level directors for zero-shot text-to-video generation. *arXiv preprint arXiv:2305.14330*, 2023. 2
- [19] Hanzhuo Huang, Yufan Feng, Cheng Shi, Lan Xu, Jingyi Yu, and Sibe Yang. Free-bloom: Zero-shot text-to-video generator with llm director and ldm animator. *Advances in Neural Information Processing Systems*, 36, 2024. 2
- [20] Ziqi Huang, Yinan He, Jiashuo Yu, Fan Zhang, Chenyang Si, Yuming Jiang, Yuanhan Zhang, Tianxing Wu, Qingyang Jin, Nattapol Chanpaisit, et al. Vbench: Comprehensive benchmark suite for video generative models. In *Proceedings of the IEEE/CVF Conference on Computer Vision and Pattern Recognition*, pages 21807–21818, 2024. 2, 5, 6, 7, 8
- [21] Yang Jin, Zhicheng Sun, Ningyuan Li, Kun Xu, Hao Jiang, Nan Zhuang, Quzhe Huang, Yang Song, Yadong Mu, and Zhouchen Lin. Pyramidal flow matching for efficient video generative modeling. *arXiv preprint arXiv:2410.05954*, 2024. 1, 2, 6, 7, 13
- [22] Yunxin Li, Haoyuan Shi, Baotian Hu, Longyue Wang, Jiashun Zhu, Jinyi Xu, Zhen Zhao, and Min Zhang. Animdirector: A large multimodal model powered agent for controllable animation video generation. *arXiv preprint arXiv:2408.09787*, 2024. 2
- [23] Yaowei Li, Xintao Wang, Zhaoyang Zhang, Zhouxia Wang, Ziyang Yuan, Liangbin Xie, Yuexian Zou, and Ying Shan. Image conductor: Precision control for interactive video synthesis. *arXiv preprint arXiv:2406.15339*, 2024. 3

- [24] Long Lian, Baifeng Shi, Adam Yala, Trevor Darrell, and Boyi Li. Llm-grounded video diffusion models. *arXiv preprint arXiv:2309.17444*, 2023. 2
- [25] Han Lin, Abhay Zala, Jaemin Cho, and Mohit Bansal. Videodirectorgpt: Consistent multi-scene video generation via llm-guided planning. *arXiv preprint arXiv:2309.15091*, 2023. 2
- [26] Haotian Liu, Chunyuan Li, Qingyang Wu, and Yong Jae Lee. Visual instruction tuning. *Advances in neural information processing systems*, 36, 2024. 2
- [27] Xinhang Liu, Yu-Wing Tai, and Chi-Keung Tang. Chatcam: Empowering camera control through conversational ai. *arXiv preprint arXiv:2409.17331*, 2024. 2
- [28] Yu Lu, Linchao Zhu, Hehe Fan, and Yi Yang. Flowzero: Zero-shot text-to-video synthesis with llm-driven dynamic scene syntax. *arXiv preprint arXiv:2311.15813*, 2023. 2
- [29] Xin Ma, Yaohui Wang, Gengyu Jia, Xinyuan Chen, Yuanfang Li, Cunjian Chen, and Yu Qiao. Cinemo: Consistent and controllable image animation with motion diffusion models. *arXiv preprint arXiv:2407.15642*, 2024. 1, 2
- [30] Yue Ma, Yingqing He, Hongfa Wang, Andong Wang, Chenyang Qi, Chengfei Cai, Xiu Li, Zhifeng Li, Heung-Yeung Shum, Wei Liu, et al. Follow-your-click: Open-domain regional image animation via short prompts. *arXiv preprint arXiv:2403.08268*, 2024. 1
- [31] Kangfu Mei and Vishal Patel. Vidm: Video implicit diffusion models. In *Proceedings of the AAAI conference on artificial intelligence*, pages 9117–9125, 2023. 1
- [32] Muyao Niu, Xiaodong Cun, Xintao Wang, Yong Zhang, Ying Shan, and Yinqiang Zheng. Mofa-video: Controllable image animation via generative motion field adaptations in frozen image-to-video diffusion model. *arXiv preprint arXiv:2405.20222*, 2024. 1, 3, 5, 8
- [33] Gyeongrok Oh, Jaehwan Jeong, Sicun Kim, Wonmin Byeon, Jinkyu Kim, Sungwoong Kim, Hyeokmin Kwon, and Sangpil Kim. Mtv: Multi-text video generation with text-to-video models. *arXiv preprint arXiv:2312.04086*, 2023. 2
- [34] OpenAI. Chatgpt. <https://openai.com/index/chatgpt>, 2022. 2, 6
- [35] William Peebles and Saining Xie. Scalable diffusion models with transformers. In *Proceedings of the IEEE/CVF International Conference on Computer Vision*, pages 4195–4205, 2023. 2
- [36] Tianhe Ren, Shilong Liu, Ailing Zeng, Jing Lin, Kunchang Li, He Cao, Jiayu Chen, Xinyu Huang, Yukang Chen, Feng Yan, et al. Grounded sam: Assembling open-world models for diverse visual tasks. *arXiv preprint arXiv:2401.14159*, 2024. 3, 8
- [37] Weiming Ren, Huan Yang, Ge Zhang, Cong Wei, Xinrun Du, Wenhao Huang, and Wenhui Chen. Consisti2v: Enhancing visual consistency for image-to-video generation. *arXiv preprint arXiv:2402.04324*, 2024. 1, 2, 5, 6
- [38] Olaf Ronneberger, Philipp Fischer, and Thomas Brox. U-net: Convolutional networks for biomedical image segmentation. In *Medical image computing and computer-assisted intervention—MICCAI 2015: 18th international conference, Munich, Germany, October 5-9, 2015, proceedings, part III 18*, pages 234–241. Springer, 2015. 2
- [39] Xiaoyu Shi, Zhaoyang Huang, Fu-Yun Wang, Weikang Bian, Dasong Li, Yi Zhang, Manyuan Zhang, Ka Chun Cheung, Simon See, Hongwei Qin, et al. Motion-i2v: Consistent and controllable image-to-video generation with explicit motion modeling. In *ACM SIGGRAPH 2024 Conference Papers*, pages 1–11, 2024. 3, 6, 7
- [40] Uriel Singer, Adam Polyak, Thomas Hayes, Xi Yin, Jie An, Songyang Zhang, Qiyuan Hu, Harry Yang, Oron Ashual, Oran Gafni, et al. Make-a-video: Text-to-video generation without text-video data. *arXiv preprint arXiv:2209.14792*, 2022. 1
- [41] Achint Soni, Sreyas Venkataraman, Abhranil Chandra, Sebastian Fischmeister, Percy Liang, Bo Dai, and Sherry Yang. Videoagent: Self-improving video generation. *arXiv preprint arXiv:2410.10076*, 2024. 2
- [42] Zhiyu Tan, Xiaomeng Yang, Luozheng Qin, and Hao Li. Vidgen-1m: A large-scale dataset for text-to-video generation. *arXiv preprint arXiv:2408.02629*, 2024. 1, 2
- [43] Rohan Taori, Ishaan Gulrajani, Tianyi Zhang, Yann Dubois, Xuechen Li, Carlos Guestrin, Percy Liang, and Tatsunori B Hashimoto. Stanford alpaca: An instruction-following llama model, 2023. 2
- [44] Vbench Team. Vbench leaderboard. https://huggingface.co/spaces/Vchitect/VBench_Leaderboard, 2024. 6
- [45] HPC-AI Tech. Open-sora. <https://github.com/hpcaitech/Open-Sora>, 2024. 2
- [46] Zachary Teed and Jia Deng. Droid-slam: Deep visual slam for monocular, stereo, and rgb-d cameras. *Advances in neural information processing systems*, 34:16558–16569, 2021. 5, 12
- [47] Ye Tian, Ling Yang, Haotian Yang, Yuan Gao, Yufan Deng, Jingmin Chen, Xintao Wang, Zhaochen Yu, Xin Tao, Pengfei Wan, et al. Videotetris: Towards compositional text-to-video generation. *arXiv preprint arXiv:2406.04277*, 2024. 2
- [48] Hugo Touvron, Thibaut Lavril, Gautier Izacard, Xavier Martinet, Marie-Anne Lachaux, Timothée Lacroix, Baptiste Rozière, Naman Goyal, Eric Hambro, Faisal Azhar, et al. Llama: Open and efficient foundation language models. *arXiv preprint arXiv:2302.13971*, 2023. 2
- [49] Yi Wang, Yinan He, Yizhuo Li, Kunchang Li, Jiashuo Yu, Xin Ma, Xinhao Li, Guo Chen, Xinyuan Chen, Yaohui Wang, et al. Internvid: A large-scale video-text dataset for multimodal understanding and generation. *arXiv preprint arXiv:2307.06942*, 2023. 1, 2
- [50] Zhouxia Wang, Ziyang Yuan, Xintao Wang, Yaowei Li, Tianshui Chen, Menghan Xia, Ping Luo, and Ying Shan. Motionctrl: A unified and flexible motion controller for video generation. In *ACM SIGGRAPH 2024 Conference Papers*, pages 1–11, 2024. 1, 3
- [51] Jianzong Wu, Xiangtai Li, Yanhong Zeng, Jiangning Zhang, Qianyu Zhou, Yining Li, Yunhai Tong, and Kai Chen. Motionbooth: Motion-aware customized text-to-video generation. *arXiv preprint arXiv:2406.17758*, 2024.
- [52] Weijia Wu, Zhuang Li, Yuchao Gu, Rui Zhao, Yefei He, David Junhao Zhang, Mike Zheng Shou, Yan Li, Tingting Gao, and Di Zhang. Draganything: Motion control for any-

- thing using entity representation. In *European Conference on Computer Vision*, pages 331–348. Springer, 2025. 1, 3
- [53] Zhifei Xie, Daniel Tang, Dingwei Tan, Jacques Klein, Tegawend F Bissyand, and Saad Ezzini. Dreamfactory: Pioneering multi-scene long video generation with a multi-agent framework. *arXiv preprint arXiv:2408.11788*, 2024. 2
- [54] Jinbo Xing, Menghan Xia, Yong Zhang, Haoxin Chen, Wangbo Yu, Hanyuan Liu, Gongye Liu, Xintao Wang, Ying Shan, and Tien-Tsin Wong. Dynamicrafter: Animating open-domain images with video diffusion priors. In *European Conference on Computer Vision*, pages 399–417. Springer, 2025. 1, 2, 5, 6, 7, 13
- [55] Dejjia Xu, Yifan Jiang, Chen Huang, Liangchen Song, Thorsten Gernoth, Liangliang Cao, Zhangyang Wang, and Hao Tang. Cavia: Camera-controllable multi-view video diffusion with view-integrated attention. *arXiv preprint arXiv:2410.10774*, 2024. 1, 2
- [56] Dejjia Xu, Weili Nie, Chao Liu, Sifei Liu, Jan Kautz, Zhangyang Wang, and Arash Vahdat. Camco: Camera-controllable 3d-consistent image-to-video generation. *arXiv preprint arXiv:2406.02509*, 2024. 1, 2
- [57] Haofei Xu, Jing Zhang, Jianfei Cai, Hamid Rezaatoughi, Fisher Yu, Dacheng Tao, and Andreas Geiger. Unifying flow, stereo and depth estimation. *IEEE Transactions on Pattern Analysis and Machine Intelligence*, 2023. 5, 12
- [58] Hongwei Xue, Tiankai Hang, Yanhong Zeng, Yuchong Sun, Bei Liu, Huan Yang, Jianlong Fu, and Baining Guo. Advancing high-resolution video-language representation with large-scale video transcriptions. In *Proceedings of the IEEE/CVF Conference on Computer Vision and Pattern Recognition*, pages 5036–5045, 2022. 1, 2
- [59] Zhengyuan Yang, Linjie Li, Kevin Lin, Jianfeng Wang, Chung-Ching Lin, Zicheng Liu, and Lijuan Wang. The dawn of lmms: Preliminary explorations with gpt-4v (ision). *arXiv preprint arXiv:2309.17421*, 9(1):1, 2023. 2
- [60] Zhuoyi Yang, Jiayan Teng, Wendi Zheng, Ming Ding, Shiyu Huang, Jiazheng Xu, Yuanming Yang, Wenyi Hong, Xiaohan Zhang, Guanyu Feng, et al. Cogvideox: Text-to-video diffusion models with an expert transformer. *arXiv preprint arXiv:2408.06072*, 2024. 1, 2, 6, 7, 13
- [61] Shengming Yin, Chenfei Wu, Jian Liang, Jie Shi, Houqiang Li, Gong Ming, and Nan Duan. Dragnuwa: Fine-grained control in video generation by integrating text, image, and trajectory. *arXiv preprint arXiv:2308.08089*, 2023. 1, 2
- [62] Wei Yin, Chi Zhang, Hao Chen, Zhipeng Cai, Gang Yu, Kaixuan Wang, Xiaozhi Chen, and Chunhua Shen. Metric3d: Towards zero-shot metric 3d prediction from a single image. In *Proceedings of the IEEE/CVF International Conference on Computer Vision*, pages 9043–9053, 2023. 4
- [63] Aohan Zeng, Xiao Liu, Zhengxiao Du, Zihan Wang, Hanyu Lai, Ming Ding, Zhuoyi Yang, Yifan Xu, Wendi Zheng, Xiao Xia, et al. Glm-130b: An open bilingual pre-trained model. *arXiv preprint arXiv:2210.02414*, 2022. 2
- [64] Xiaohang Zhan, Xingang Pan, Ziwei Liu, Dahua Lin, and Chen Change Loy. Self-supervised learning via conditional motion propagation. In *Proceedings of the IEEE/CVF Conference on Computer Vision and Pattern Recognition*, pages 1881–1889, 2019. 4, 5, 13
- [65] Chi Zhang, Zhao Yang, Jiaxuan Liu, Yucheng Han, Xin Chen, Zebiao Huang, Bin Fu, and Gang Yu. Appagent: Multimodal agents as smartphone users. *arXiv preprint arXiv:2312.13771*, 2023. 3, 12
- [66] David Junhao Zhang, Dongxu Li, Hung Le, Mike Zheng Shou, Caiming Xiong, and Doyen Sahoo. Moonshot: Towards controllable video generation and editing with multimodal conditions. *arXiv preprint arXiv:2401.01827*, 2024. 1, 2
- [67] Hang Zhang, Xin Li, and Lidong Bing. Video-llama: An instruction-tuned audio-visual language model for video understanding. *arXiv preprint arXiv:2306.02858*, 2023. 2
- [68] Shiwei Zhang, Jiayu Wang, Yingya Zhang, Kang Zhao, Hangjie Yuan, Zhiwu Qin, Xiang Wang, Deli Zhao, and Jingren Zhou. I2vgen-xl: High-quality image-to-video synthesis via cascaded diffusion models. *arXiv preprint arXiv:2311.04145*, 2023. 1, 2, 5, 6
- [69] Zhenghao Zhang, Junchao Liao, Menghao Li, Long Qin, and Weizhi Wang. Tora: Trajectory-oriented diffusion transformer for video generation. *arXiv preprint arXiv:2407.21705*, 2024. 1, 2
- [70] Peng Zheng, Dehong Gao, Deng-Ping Fan, Li Liu, Jorma Laaksonen, Wanli Ouyang, and Nicu Sebe. Bilateral reference for high-resolution dichotomous image segmentation. *CAAI Artificial Intelligence Research*, 3:9150038, 2024. 12
- [71] Haitao Zhou, Chuang Wang, Rui Nie, Jinxiao Lin, Dongdong Yu, Qian Yu, and Changhu Wang. Trackgo: A flexible and efficient method for controllable video generation. *arXiv preprint arXiv:2408.11475*, 2024. 1, 3
- [72] Shaobin Zhuang, Kunchang Li, Xinyuan Chen, Yaohui Wang, Ziwei Liu, Yu Qiao, and Yali Wang. Vlogger: Make your dream a vlog. In *Proceedings of the IEEE/CVF Conference on Computer Vision and Pattern Recognition*, pages 8806–8817, 2024. 2

MotionAgent: Fine-grained Controllable Video Generation via Motion Field Agent

Supplementary Material

6. Object Trajectory Plotting Module

6.1. Details of Trajectory Plotting

Inspired by AppAgent [65], we replace direct trajectory generation with grid selection based on grid numbers. Specifically, we divide the given image into $N \times M$ grids, breaking it down into small square areas. Each area is labeled with an integer in the top-left corner and subdivided into nine subareas. Based on the previous step, we identify the starting point of the trajectory using the detection result and plot this starting point on the image, represented by a circle. Then, we provide the image overlaid with the grids and starting point as input to the agent.

We define the following functions: *Set_*.Points* (*start: int, string; mid_*.: int, string; end: int, string*) for the agent. Here, * is an integer ranging from 1 – 4, used to achieve varying lengths and curvature in trajectory plotting. The parameters *start*, *mid_**, and *end* include an integer label assigned to the grid area and a string representing the exact location within the grid area. The string can take one of the following nine values: center, top-left, top, top-right, left, right, bottom-left, bottom, and bottom-right.

A simple use case is *Set_2.Points* (*start: 143, top-right; end: 33, bottom-right*), which sets the starting point of the trajectory at the top-right of grid area 143 and the endpoint at the bottom-right of grid area 33. As illustrated in Figure 6, this function represents a simple linear trajectory.

Once we obtain the complete object trajectory, we use interpolation to determine the position in the trajectory for each frame. Then, these interpolated positions are input into the subsequent model to calculate dense optical flow.

6.2. More Ablation Study

Here, we conduct an ablation study on different approaches for trajectory plotting. We use direct offset generation as the

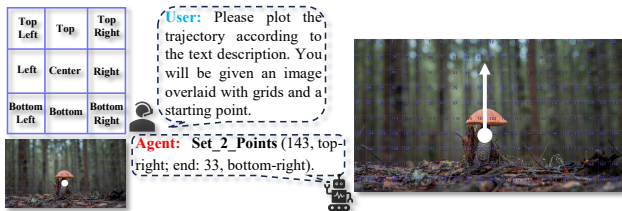


Figure 6. Details of trajectory plotting: The grid divides the image into small square areas. Each area is labeled with an integer in the top-left corner and is further subdivided into nine subareas.

Offset Generation	Grid Selection	Object Movement Q&A	Dynamic Degree
✓	✓	29.28	7.63
		45.69	32.11

Table 4. Ablation study of trajectory plotting module (all values are in percentage).

baseline module instead of grid selection. Specifically, we provide the agent with the starting point location based on the detection results and ask the agent to directly generate offsets from the starting point to define the object trajectory.

As shown in Table 4, the grid selection approach shows better evaluation results in both metrics. The grid selection approach gives the agent an overall understanding of the image layout, and it is easier for the agent to use than direct offset generation. As for the dynamic degree metrics, the offset generation approach cannot output a suitable trajectory length, which may lead to a lower dynamic degree.

7. Training Data Preparation

To eliminate the domain gap between the unified and real optical flow maps, we propose fine-tuning the optical flow adapter module, which maintains the generation capabilities of the base I2V diffusion model. For each video used for training, we first utilize a binary segmentation model, BiRefNet [70], to decompose the foreground and background. We then remove the dynamic foreground based on the binary segmentation mask. Next, we adopt an SLAM method, DROID-SLAM [46], to compute the camera extrinsics \hat{E} for each frame based on the masked video. Additionally, for the original video, we use an optical flow model, Unimatch [57], to estimate the real optical flow \hat{F} .

Next, we explain how to estimate the optical flow caused by object movement based on the camera extrinsics \hat{E} and real optical flow \hat{F} . We define I^0 as the pixel position in the first frame. According to the predicted real optical flow \hat{F} , we compute the corresponding pixel position in the following frames, which can be formulated as:

$$\hat{I} = I^0 + \hat{F}. \quad (5)$$

We reproject the pixel position in the following frames back to the first frame based on the predicted camera extrinsics \hat{E} . This can be computed by:

$$\hat{I}^0 = \Pi(\hat{E}^{-1}\Pi^{-1}(\hat{I})), \quad (6)$$

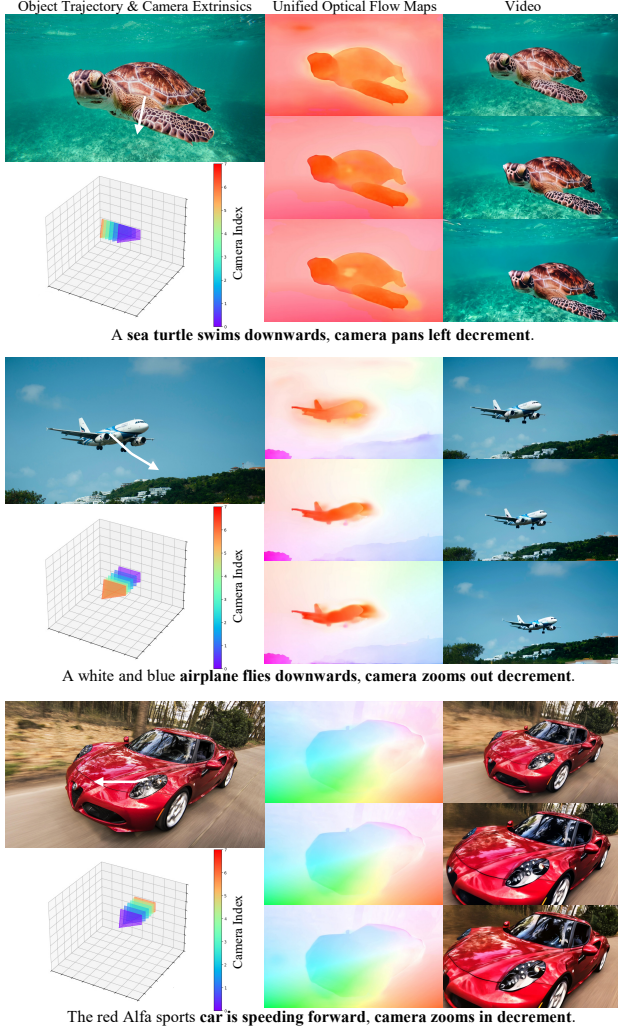


Figure 7. Intermediate representations generation by motion field agent, including object trajectory, camera extrinsics, and unified optical flow maps.

where Π and Π^{-1} are the projection and unprojection operations, respectively. \hat{I}^0 indicates the pixel position in the first frame that contains only object movement. Finally, we compute the optical flow caused by object movement:

$$\hat{F}_{obj} = \hat{I}^0 - I^0. \quad (7)$$

We perform sampling [64] on these optical flow maps of object movement to obtain sparse object trajectories. Subsequently, we reuse the proposed analytical composition method to calculate the unified optical flow maps \bar{F} , which are utilized as input to fine-tune the optical flow adapter. Additionally, we calculate the error between the unified optical flow maps \bar{F} and the real optical flow \hat{F} . If the error exceeds a threshold, we replace the unified optical flow maps \bar{F} with the real optical flow \hat{F} for training.

8. Qualitative Results

8.1. Visualization of Intermediate Representations

As illustrated in Figure 7, we show the intermediate representations generation by the motion field agent.

8.2. More Comparison Results

In Figure 8, we show more results compared to DynamicCrafter [54], CogVideoX [60] and Pyramid Flow [21].

9. User Study Interface

Figure 9 shows the designed user study interface. For each question, we randomly shuffle four videos generated by our method and the other three methods. We then ask participants to rank the videos from highest to lowest twice based on specific requirements. After the user study, we calculate the mean ranking for each method across different evaluation dimensions.

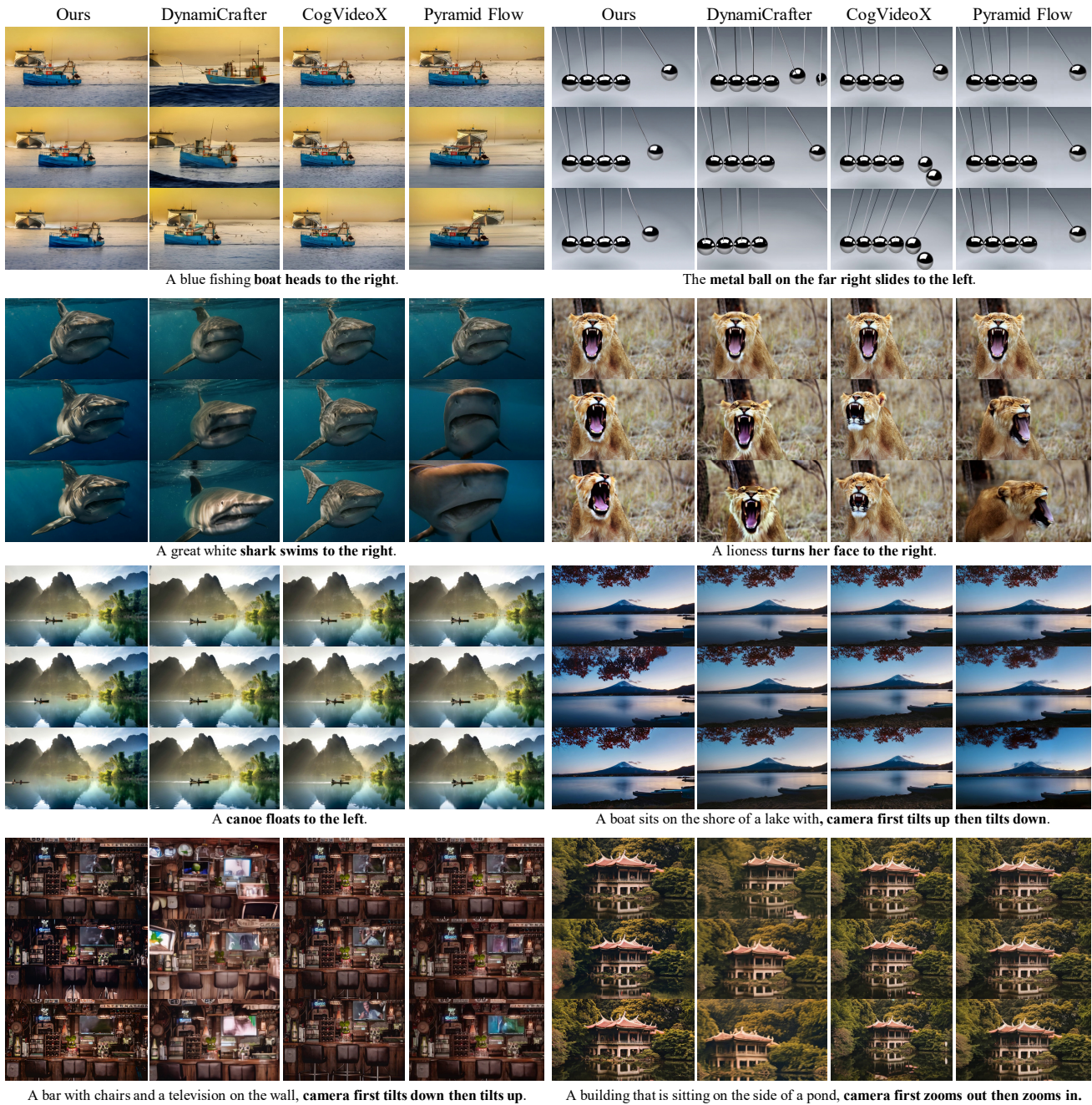


Figure 8. More comparison results of controllable I2V generation on our benchmark. The motion described in the text is in **bold**.

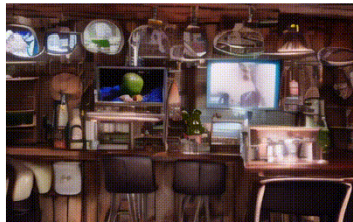
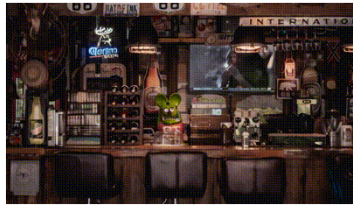
User Study on Controllable I2V Generation

Below are four videos per group. Please sort each group twice according to the following two criteria.

Criteria 1: Please sort the videos by visual quality from best to worst.

Criteria 2: Please sort the videos from high to low based on the semantic alignment of the motion information in the text prompt and the video.

* **01** Please sort the videos by visual quality from best to worst.



Video 1	
Video 2	
Video 3	
Video 4	

* **02** Please sort the videos from high to low based on the semantic alignment of the motion information in the text prompt and the video.

Text Prompt: "a bar with chairs and a television on the wall, camera first tilts down then tilts up."

Video 1	
Video 2	
Video 3	
Video 4	

Figure 9. User study interface. Each participant is required to evaluate 30 groups of videos and respond to two corresponding sub-questions for each group. Due to the page limit, only one group of videos and two sub-questions are shown here.